

Acid Leaching of SHS Produced Magnesium Oxide/Titanium Diboride

Jonathan Y. Lok,[‡] Kathryn V. Logan,^{*,**,*†} and Jairaj J. Payyapilly*

Department of Materials Science and Engineering, Virginia Polytechnic and State University, Blacksburg, Virginia 24060

The stoichiometric self-propagating high-temperature synthesis (SHS) thermite reaction involving magnesium (Mg), titanium dioxide (TiO₂), and boron oxide (B₂O₃) forms MgO and titanium diboride (TiB₂) as final products. Selective acid leaching is used to remove the MgO leaving TiB₂ powder. This study investigates the acid leaching of SHS-produced MgO/TiB₂ powders and a stoichiometric mixture of commercially obtained MgO and TiB₂ powders. Leaching was conducted at pH levels of 4.0, 2.5, and 1.0 by the introduction of concentrated aliquots of HNO₃. This method maintains a minimum pH target throughout the leaching process, thereby sustaining a dynamic concentration to remove the oxide. The optimal leaching conditions were determined to be at 90°C at a minimum pH target of 2.5 for the SHS-produced product. At these conditions, conversion percentages of 83%–84% of MgO were measured with only trace amounts of TiB₂ measured in the solution (<100 µg/L). Conversion percentages for each leaching condition and dissolution mass of solid MgO and TiB₂ at each pH are also reported. Results from powder X-ray diffraction confirm the removal of MgO and minimal dissolution of TiB₂, and indicate the formation of unidentified compounds. Inductively coupled plasma mass spectrometry (ICP) was used to analyze the ionic composition and extent of leaching. Scanning electron microscopy was used to observe the particle morphology of the leached powders.

I. Introduction

TITANIUM diboride is a refractory ceramic known for its high hardness, strength to density ratio, and wear resistance.¹ Potential applications include wear-resistant coatings and ballistic armor. Industries are interested in TiB₂ for its chemical/environmental passivity, tribological properties, electrical conductivity, and thermal shock resistance.² Of the various methods to synthesize TiB₂, carbothermic/borothermic reduction and self-propagating high-temperature synthesis (SHS) are the most prevalent. Recent works by others^{3–7} have investigated cold milling, rapid carbothermic reduction, and single-step boronation as low-energy alternatives. Commercially, carbothermic and borothermic reduction is used to reduce rutile TiO₂ to produce TiB₂. While exhibiting excellent control of reaction dynamics, the carbothermic and borothermic reduction pathways are energy intensive. They are kinetically favorable above 2000° and 1200°C, respectively.^{8,9} The magnesium SHS method to synthesize TiB₂ is a fast, low-energy alternative. The overall reaction is shown in Eq. (1).



Stoichiometric amounts of the reactants are intimately mixed and reacted in a silica crucible. A resistance heated NiCr wire is used to initiate the reaction with a variable transformer. The reaction requires a relatively low-energy input and takes <1 min to complete. The products formed by Eq. (1) consist of an agglomerated MgO encasing TiB₂ platelets that must be broken up to facilitate the removal of MgO.¹⁰

Classical handbook literature by Samsonov *et al.* and more recent work by Sangwal *et al.* have compared the kinetics of MgO dissolution and TiB₂ yield amongst various acids. Strong acids are thermodynamically more favorable than weak acids or electrolyte solutions. Of the strong acids, nitric acid had the highest TiB₂ yield over a range of concentrations and temperatures. Others have leached the MgO/TiB₂ products with strong acids, particularly H₂SO₄, HCl, and HNO₃.^{11–16} Leaching with HCl in particular resulted in a pyrophoric product, possibly due to the higher surface area that was produced from dissolution of particles at the nanoscale level.¹⁰ Others have reported the use of HCl with varying results, showing both excessive and acceptable losses of TiB₂.^{17,18} Quantified results of the dissolution of TiB₂ have not been found in the literature.

II. Experimental Procedure

(1) Synthesis

Stoichiometric amounts of reactant powders were mixed according to Eq. (1). Three, 130.0 g batches (96.7 g MgO and 33.3 g TiB₂ theoretical yield) were mixed to produce all powders used in this study. Pigment grade TiO₂ anatase (38.3 g, 1.0 µm mean particle size) and B₂O₃ (33.4 g, 189.5 µm mean particle size), both from Fisher Scientific (Fair Lawn, NJ), were weighed and mixed in an alumina mortar and pestle with a light shearing motion. Once homogenized, 58.3 g (643.7 µm mean particle size) of Mg flakes from Reade Manufacturing (Manchester, NJ) were added to the mortar. The powders were completely homogenized when a light-gray appearance of the mixture was achieved. The mixture was transferred to a slip cast fused silica crucible, and placed in an enclosed, air-tight, refractory-lined reaction chamber. A second crucible was placed on top of the first crucible with a 1 kg weight to retain the powders within the closed system. To initiate the reaction, a NiCr wire was connected to a variable transformer (12 A, 120 V). The wire was placed in the crucible, just touching the top of the reactant powders. The voltage was increased at a rate of about 2.5 V/5 s.

(2) Processing

The cemented MgO/TiB₂ agglomerates were ball milled to break apart the reacted mass in preparation for acid leaching. A 4.9 L Type 304 stainless steel mill jar and 1.27 cm Type 302/304 stainless steel balls were used for milling. The particle size effect of acid leaching is not considered a part of the scope of this work, and is a fixed parameter. Previous work showed no further reduction in SHS MgO/TiB₂ agglomerate size after 18–20 h of

T. Besmann—contributing editor

Manuscript No. 24270. Received January 27, 2008; approved October 15, 2008.

Presented at The 31st International Cocoa Beach Conference and Exposition on Advanced Ceramics & Composites (ICACC), Daytona Beach, FL.

Work was funded by a grant from the National Institute of Aerospace (Grant Award No.: VT-03-01).

*Member, The American Ceramic Society.

**Fellow, The American Ceramic Society, 1992.

†Present address: Exxon Mobil Research and Engineering, Materials Engineering, Fairfax, VA 22037.

‡Author to whom correspondence should be addressed. e-mail: jairajp@vt.edu

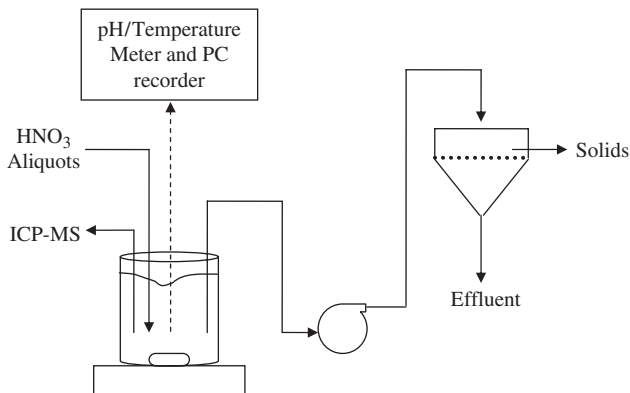


Fig. 1. Acid leaching and filtration apparatus.

milling, so the reaction products were dried in an oven at 110°C for 12 h and milled for 20 h.

(3) Testing

Leaching was performed by the addition of concentrated aliquots of HNO₃. Three minimum pH targets (4.0, 2.5, and 1.0) were selected to see the effects on the dissolution and morphology of TiB₂. This technique of leaching MgO allowed for minimal dissolution of TiB₂, and correlates the point at which TiB₂ appears in solution to the moles of acid in the system. As the system approached neutrality, an aliquot of acid was introduced, driving the pH down to the target level. Consequently, the pH of the solution behaves like a buffer, with characteristic sawtooth oscillations with time.

Two sources of powders were used for leaching, a stoichiometric mixture of commercially available MgO and TiB₂, and the MgO/TiB₂ product synthesized by SHS. Three temperature levels were used to leach the commercial powders, 90°, 60°, and 30°C. There was no difference in rate by the addition of aliquots between 90°C and the experiments at 60° and 30°C. Therefore 90°C was selected for the leaching of the SHS products.

A second leaching cycle was performed on the SHS powders to observe if the saturation limit of Mg(NO₃)₂ was inhibiting the reaction of MgO or Mg(OH)₂ with HNO₃. Special regard was given to a decrease in solubility due to a common ion effect with NO₃⁻ from the dissociation of HNO₃. During the leaching process, samples of the solution were filtered through a 0.45 μm syringe filter for ICP-MS analysis at predetermined HNO₃ volumes. At the end of the leaching cycle, the solution was pumped to a vacuum-assisted filtration apparatus, shown in Fig. 1. A 0.2 μm filter was used for solids recovery, and the liquid effluent was discarded. The recovered solids were dried in an oven at 110°C for scanning electron microscopy (SEM)/energy-dispersed X-ray spectroscopy (EDS) and powder X-ray diffraction (XRD) analysis.

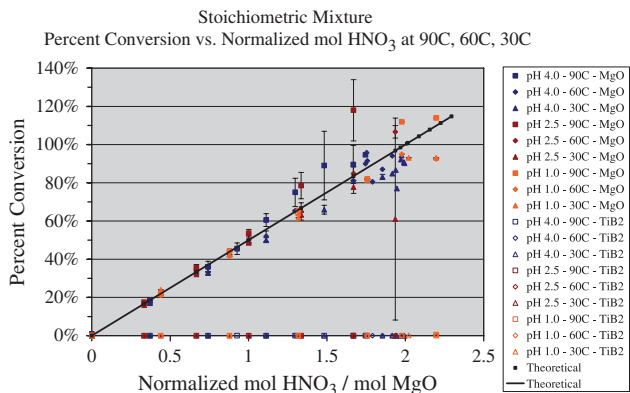


Fig. 2. Conversion percentage of the commercial mixture of MgO and TiB₂ from ICP-MS.

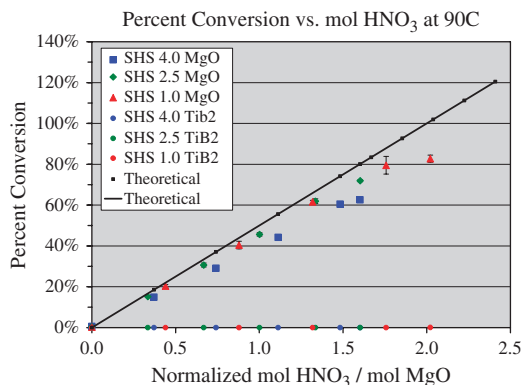


Fig. 3. Conversion percentage of self-propagating high-temperature synthesis produced MgO/TiB₂ from ICP-MS.

(4) Characterization

For liquids analysis, an X-Series Thermo Electron ICP-MS was used to determine the ion concentrations of ²⁵Mg, ⁴⁷Ti, and ⁴⁸Ti ions. Each sample was diluted to a maximum of 100 μg/L of the highest concentration ion. To analyze the final products, a Jeol JSM-6400 (Peabody, MA) SEM with EDAX EDS and a LEO 1550 field emission SEM (Thornwood, NY) equipped with a Gemini column were used to observe the particle size and morphology of the solids. All samples were thickness-controlled sputter coated to 15 nm with gold-palladium. Powder XRD was performed on a Siemens D5000 Diffractometer (New York, NY) running Diffrac^{plus} EVA software for diffraction evaluation. Dried powders were mounted on the stage with methanol to avoid preferred orientation. A standard CuKα diffraction pattern was produced scanning from 18° to 104° (2 θ), with a step size of 0.01° at 2 s per step.

(5) Percent Conversion Determination

The aqueous concentration of ionic species determined by ICP analysis was also used to derive the percent conversion. The concentration of Mg and Ti ions present in the aqueous solution was used to determine the moles of reactant through the stoichiometric ratio given in Eq. (1).

III. Results and Discussion

(1) Percent Conversion and Dissolution of Products

ICP-MS results show <100 μg/L of Ti ions in the aqueous phase for all temperature and pH levels. This behavior was observed for both the commercial and the SHS-produced powders. This was due to the relatively low concentrations of acid (0.0001M–0.01M) in the leaching solution compared with methods used by others (1.0M–6.0M). The concentrations of Mg ions were also measured and compared with the theoretical 1:2

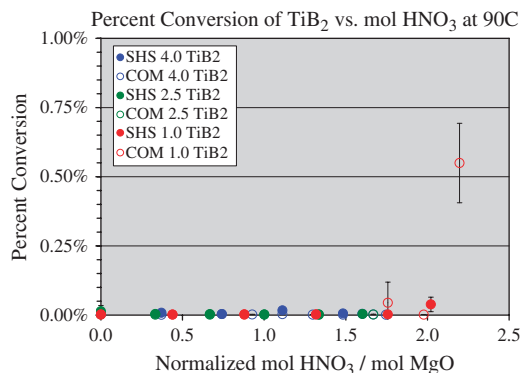


Fig. 4. Conversion of TiB₂ from leaching commercial and self-propagating high-temperature synthesis powders at 90°C.

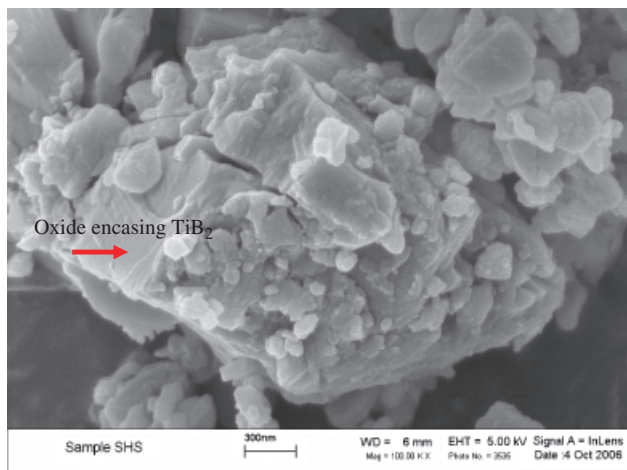
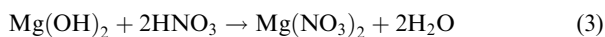
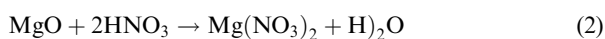


Fig. 5. As-milled self-propagating high-temperature synthesis MgO/TiB₂ before leaching.

mol ratio conversion between MgO/Mg(OH)₂ and HNO₃, shown in the following equations:



Figures 2–4 show the percent conversion of MgO and TiB₂ based on ICP-MS concentrations plotted against normalized moles of HNO₃ added to the system. The solid line represents the stoichiometric conversion into Mg(NO₃)₂. Plotting the MgO conversion illustrates the ability to achieve complete conversion, indicating the saturation point was not reached. This validates the solubility and acid–base equilibrium calculations that

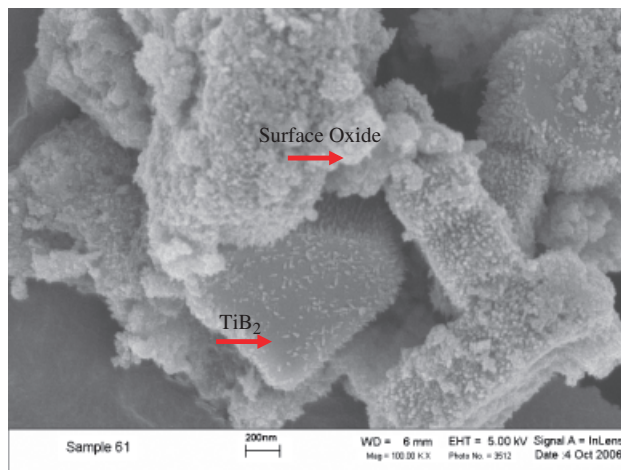


Fig. 6. Self-propagating high-temperature synthesis TiB₂ leached at minimum pH 4.0 at 90°C.

predicted the formation of Mg(NO₃)₂ was not inhibited by a saturated condition or the common ion effect.

(2) SEM/EDS

SEM micrographs and EDS spectra were taken of the SHS powders leached at 90°C for each pH target. The accompanying EDS spectra show varying degrees of oxides left in the sample. Figure 5 shows the as-milled powders and MgO encasing TiB₂ platelets even after 20 h of milling. Figures 6–11 are micrographs taken after each leaching cycle. Leaching at a minimum pH level of 2.5 appeared to have optimal results for MgO dissolution and TiB₂ retention.

The surface features shown in the pH 4.0 and 2.5 SEM images appear to be oxide derivatives present after 80% leaching. The

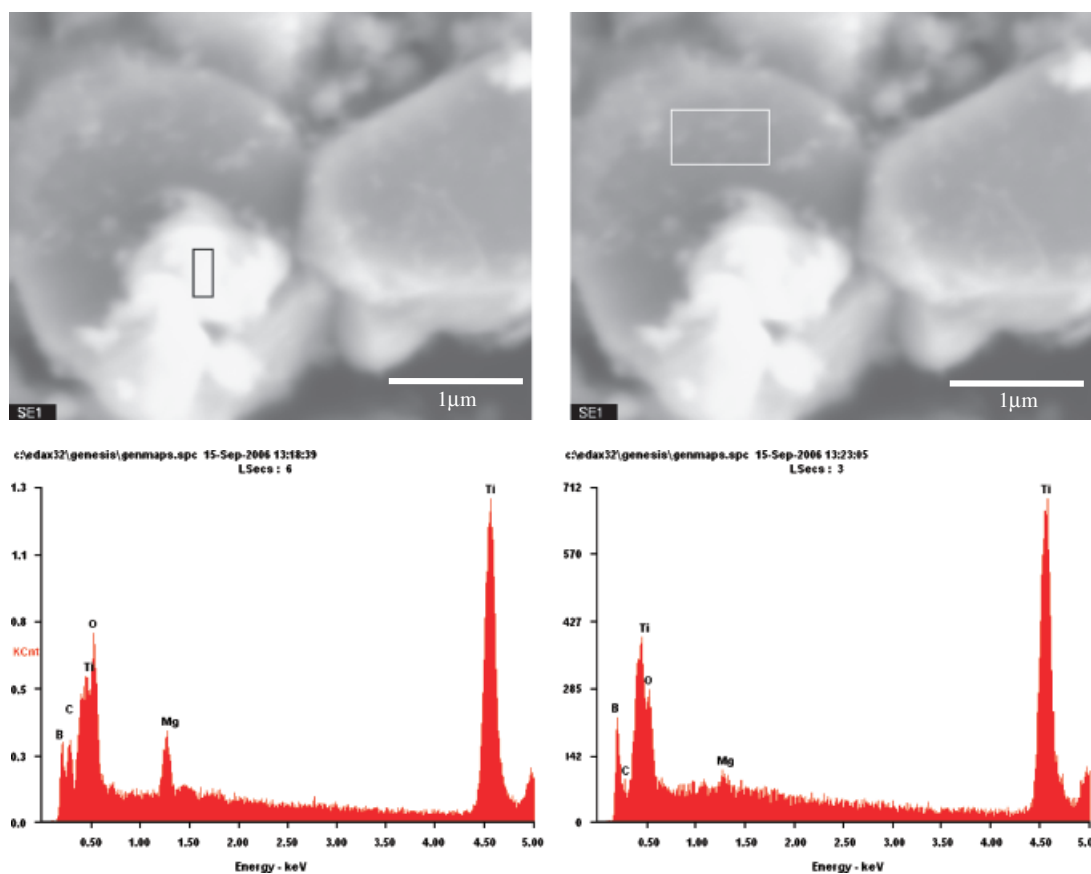


Fig. 7. Energy-dispersed X-ray spectroscopy spectra of self-propagating high-temperature synthesis TiB₂ leached at minimum pH 4.0 at 90°C.

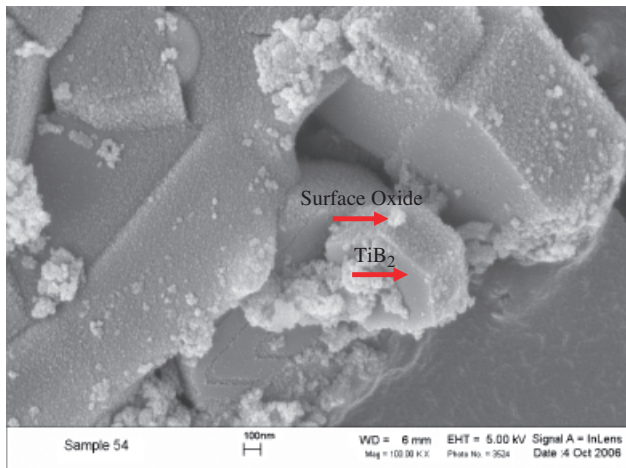


Fig. 8. Self-propagating high-temperature synthesis TiB₂ leached at minimum pH 2.5 at 90°C.

features present at each pH target indicate that TiB₂ had been converted at varying degrees. In the pH 4.0 case, unidentified compounds cover the surface, making observation of the surface texture not possible. For the pH 2.5 target, the surface texture shows evidence of apparent TiB₂ pitting. The minimum pH 1.0 case shows similar unidentified compounds on the surface.

(3) XRD

Powder XRD was used to determine the evidence of byproducts from acid leaching. A standard CuK α pattern shows the relative amounts of MgO and TiB₂ as the powders were leached. The MgO and TiB₂ peaks have been identified and indexed in Fig. 12.

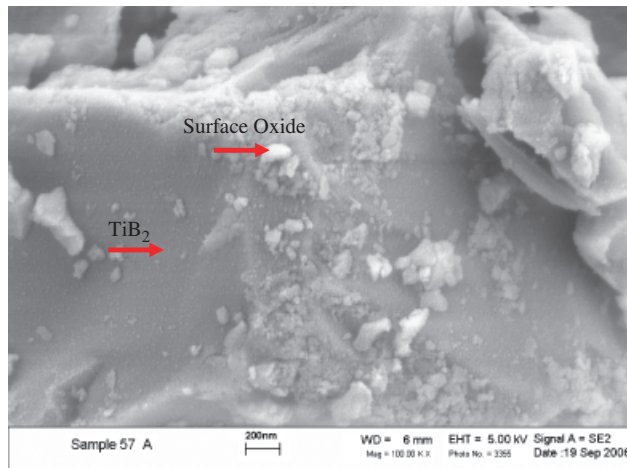


Fig. 10. Self-propagating high-temperature synthesis TiB₂ leached at minimum pH 1.0 at 90°C.

The MgO (200) and (111) planes in each case were not completely diminished, indicating that MgO was not completely leached. At a minimum pH of 4.0 and 2.5, this was expected since acid additions were performed until 80% of theoretical conversion. In the minimum pH 1.0 tests, HNO₃ was added until the pH did not change significantly. This suggests that agglomerates were affecting the leaching rate. The unidentified broadening feature at 26° (2 θ) in each of the second leaching cycle scans shows the presence of an amorphous compound or species at the nanometer scale. This feature was also present in the first leaching cycle at the pH 1.0 target.

The lack of Ti ions from ICP-MS analysis, the unidentified broad peak, and the relative reduction in the TiB₂ (101) and (100) planes indicate that a conversion of TiB₂ into an unidentified solid compound occurred. This behavior was observed

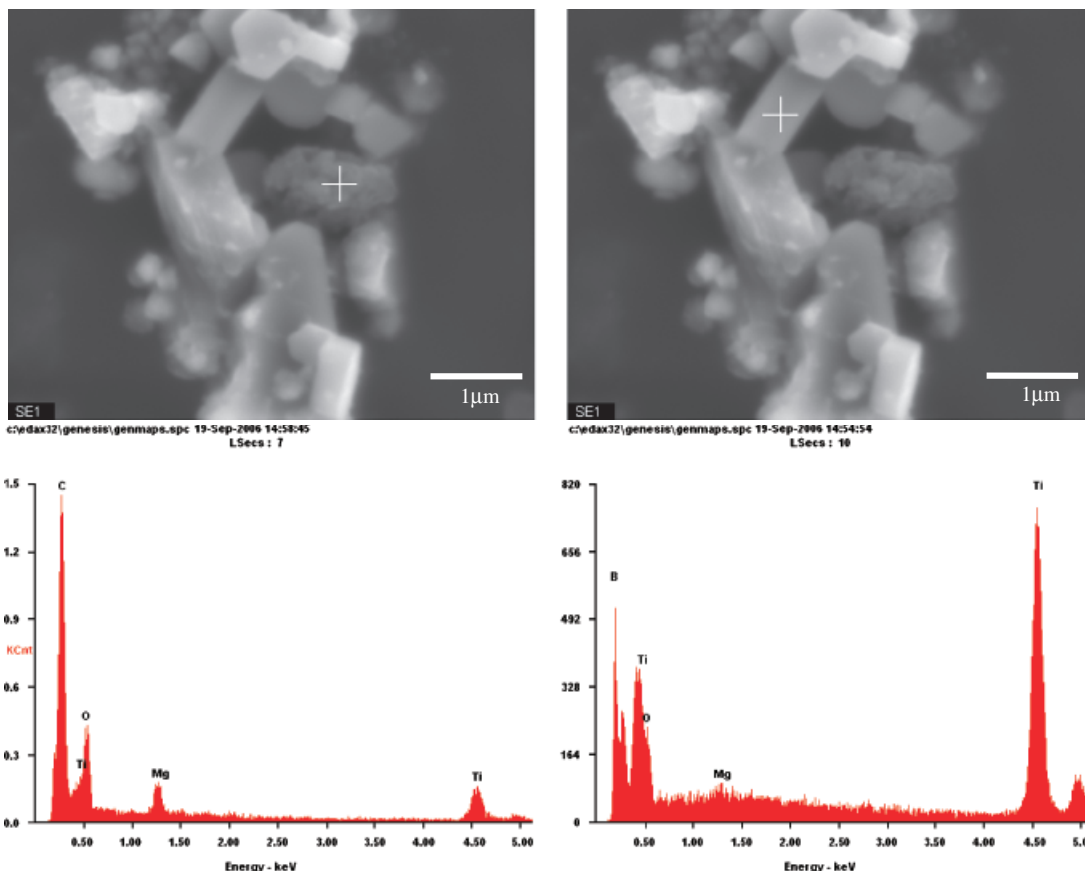


Fig. 9. Energy-dispersed X-ray spectroscopy spectra of self-propagating high-temperature synthesis TiB₂ leached at minimum pH 2.5 at 90°C.

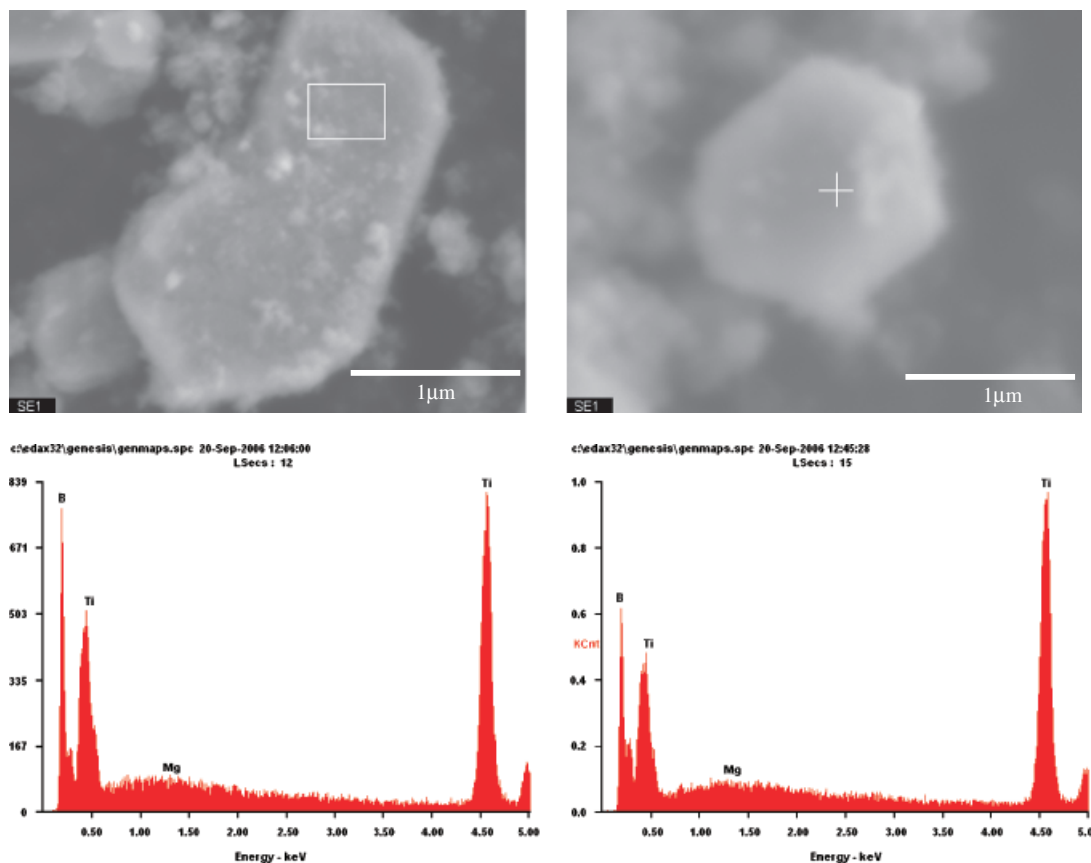


Fig. 11. Energy-dispersed X-ray spectroscopy spectra of self-propagating high-temperature synthesis TiB_2 leached at minimum pH 1.0 at 90°C .

during the second leaching cycle for all samples, and during the first leaching at a minimum pH of 1.0.

IV. Conclusion

It was determined that pure TiB_2 exhibited virtually no dissolution when leached with HNO_3 at the prescribed temperatures and pH targets. Relative low concentrations of strong acid

leaching could effectively remove 83%–84% of the MgO by-product. Optimal leaching conditions were determined to be at 90°C with a minimum pH of 2.5. This resulted in 83%–84% conversion of MgO, and $<100\ \mu\text{g/L}$ of TiB_2 in solution after one leaching cycle. A second leaching cycle incrementally increased the MgO conversion, and did not result in significant dissolution of TiB_2 . The experiments were allowed to leach until specific trends could be established. Precipitation and the com-

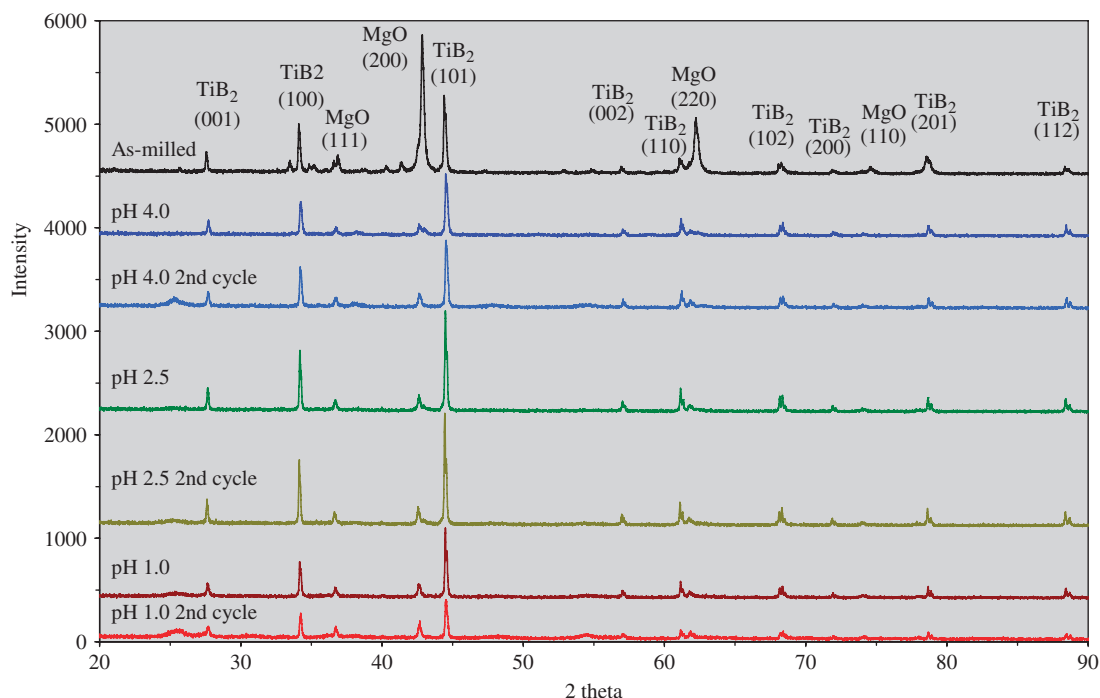


Fig. 12. Diffraction summary of all scans with respect to the as-milled self-propagating high-temperature synthesis product.

mon ion effect did not impact the solubility of the aqueous salt, nor did it hamper the dissolution of the unwanted products. This was because of the relative solubility differences in the leaching candidate chosen for the particular system.

Powder XRD revealed the formation of an unidentified compound. The relative reduction in the (101) and (100) planes revealed that TiB_2 reacted with the nitric acid, particularly during the second leaching cycle.

References

- ¹R. G. Munro, "Material Properties of Titanium Diboride," *J. Res. Nat. Inst. Standards Technol.*, **105** [5] 709–20 (2000).
- ²V. Sundaram, K. V. Logan, and R. F. Speyer, "Reaction Path in the Magnesium Thermite Reaction to Synthesize Titanium Diboride," *J. Mater. Res.*, **12** [10] 2657–64 (1997).
- ³L. Y. Chen, Y. L. Gu, Y. T. Qian, L. Shi, Z. H. Yang, and J. H. Ma, "A Facile One-Step Route to Nanocrystalline TiB_2 Powders," *Mater. Res. Bull.*, **39** [4–5] 609–13 (2004).
- ⁴R. Ricceri and P. Matteazzi, "A Fast and Low-Cost Room Temperature Process for TiB_2 Formation by Mechano-synthesis," *Mater. Sci. Eng. A-Struct. Mater. Properties Microstruct. Proc.*, **379** [1–2] 341–6 (2004).
- ⁵L. Shi, Y. L. Gu, L. Y. Chen, Z. H. Yang, J. H. Ma, and Y. T. Qian, "A Convenient Solid-State Reaction Route to Nanocrystalline TiB_2 ," *Inorg. Chem. Commun.*, **7** [2] 192–4 (2004).
- ⁶N. J. Welham, "Formation of TiB_2 from Rutile by Room Temperature Ball Milling," *Miner. Eng.*, **12** [10] 1213–24 (1999).
- ⁷N. J. Welham and D. J. Llewellyn, "Formation of Nanometric Hard Materials by Cold Milling," *J. Eur. Ceram. Soc.*, **19** [16] 2833–41 (1999).
- ⁸J. J. Kim and C. H. McMurthy, " TiB_2 Powder Production for Engineered Ceramics," *Ceram. Eng. Sci. Proc.*, **6** [9–10] 1313–20 (1985).
- ⁹J. K. Walker, "Synthesis of TiB_2 by the Borothermic Carbothermic Reduction of TiO_2 with B_4C ," *Adv. Ceram. Mater.*, **3** [6] 601–4 (1988).
- ¹⁰K. V. Logan Private Communication (2006).
- ¹¹G. V. Samsonov, *Handbook of Refractory Compounds*. IFI/Plenum, New York, 1980.
- ¹²G. V. Samsonov, *The Oxide Handbook*. IFI/Plenum, New York, 1982.
- ¹³K. Sangwal, "Dissolution Kinetics of MgO Crystals in Aqueous Acidic Salt-Solutions," *J. Mater. Sci.*, **17** [12] 3598–610 (1982).
- ¹⁴K. Sangwal, "Mechanism of Dissolution of MgO Crystals in Acids," *J. Mater. Sci.*, **15** [1] 237–46 (1980).
- ¹⁵K. Sangwal and S. K. Arora, "Etching of MgO Crystals in Acids—Kinetics and Mechanism of Dissolution," *J. Mater. Sci.*, **13** [9] 1977–85 (1978).
- ¹⁶K. Sangwal and T. C. Patel, "Etching Behavior to MgO Crystals in Relation to Chemical-Reactions," *Kristall Und Technik-Cryst. Res. Technol.*, **13** [12] 1407–12 (1978).
- ¹⁷F. Delmas, L. Goncalves, I. Martins, and M. Oliveira, "Magnesium Removal from TiC- TiB_2 SHS Powders by Controlled Hot Acid Leaching," *Adv. Mater. Forum III, Parts 1 and 2*, 594–8 (2006).
- ¹⁸N. J. Welham, "Formation of Nanometric TiB_2 from TiO_2 ," *J. Am. Ceram. Soc.*, **83** [5] 1290–2 (2000). □